

Synthesis of Substituted Pyrrole Derivatives Based on 8-Azaspiro[5.6]dodec-10-ene Scaffold

Ildar R. Iusupov¹, Victor A. Tafeenko¹, Andrea Altieri^{1,2}  and Alexander V. Kurkin^{1,*} 

¹ Department of Chemistry, Lomonosov Moscow State University, Moscow 119234, Russia; darik995@mail.ru (I.R.I.); tafeenko-victor@yandex.ru (V.A.T.); aaltieri@edasascientific.com (A.A.)

² EDASA Scientific srls, Via Stingi 37, 66050 San Salvo, Italy

* Correspondence: kurkin@direction.chem.msu.ru; Tel.: +7-495-939-22-88

Abstract: This work describes the synthesis of spirocyclic compounds based on 8-azaspiro[5.6]dodec-10-ene. Diastereomerically pure pyrrole derivatives were prepared from the spirocyclic 1,2,3-triazole using a coupling reaction. The resulting compounds were characterized via ¹H and ¹³C NMR spectroscopy and HRMS, and the crystallographic characteristics of one of them were studied via X-ray diffraction.

Keywords: spirocycle; pyrrole; 1,2,3-triazole; azaspiro

1. Introduction

Cancer is one of the most fatal diseases in the world. Millions of cases of cancer are diagnosed every year, and cancer also causes the death of millions of people. Many factors lead to the cancer generation, including, for example, environmental or heredity influences [1]. There are two main problems with anticancer drugs: non-selectivity for cancer cells and drug resistance. According to the literature, most anticancer drugs that were FDA-approved between 2010 and 2015 contain a N-heterocycle in their chemical structure [2].

Nowadays, heterocyclic chemistry has a fundamental role in drug discovery. Pyrrole derivatives are of great importance in drug design [3]. Pyrrole-based compounds have a wide range of biological activity. Among them are derivatives with properties such as anticancer [4,5], antiviral [6], antidiabetic [7], anti-inflammatory [8], etc.

Figure 1 shows some pyrrole derivatives that exhibit anticancer activity. Sunitinib (1) is a multitargeted tyrosine kinase inhibitor and is used for the treatment of two types of cancer: renal cell carcinoma (RCC) and imatinib-resistant gastrointestinal stromal tumor (GIST) [9,10]. Compound 2 is a strong inhibitor of tubulin polymerization and cancer cell growth, specifically, of the P-glycoprotein-overexpressing NCI-ADR-RES and Messa/Dx5MDR cell lines [11]. Ulixertinib (3) is a pyrrole-based protein kinase inhibitor with high potency and selectivity for ERK1/2 (extracellular signal-regulated protein kinase) and is approved for the treatment of cancer [12]. Therefore, it is not surprising that, from a statistical analysis of the presence of this ring in known drugs and natural products, it was found to be among the top ten rings and is therefore considered a privileged motif for drug design [13,14].

In addition, nowadays, scaffold rigidification is one of the most sought after strategies by medicinal chemists for the design and realization of new drug generations [15]. Although saturated rings and planar aromatic rings can influence ligand-binding entropy, it has been suggested that compounds with too many planar rings have suboptimal physical properties [16,17].



Citation: Iusupov, I.R.; Tafeenko, V.A.; Altieri, A.; Kurkin, A.V. Synthesis of Substituted Pyrrole Derivatives Based on 8-Azaspiro[5.6]dodec-10-ene Scaffold. *Molbank* **2024**, *2024*, M1765. <https://doi.org/10.3390/M1765>

Academic Editor: Hideto Miyabe

Received: 21 December 2023

Revised: 18 January 2024

Accepted: 23 January 2024

Published: 25 January 2024



Copyright: © 2024 by the authors. Licensee MDPI, Basel, Switzerland. This article is an open access article distributed under the terms and conditions of the Creative Commons Attribution (CC BY) license (<https://creativecommons.org/licenses/by/4.0/>).

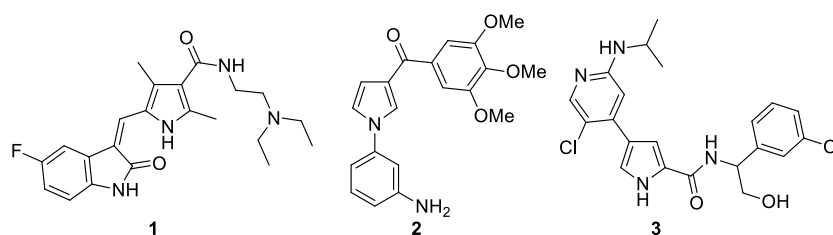
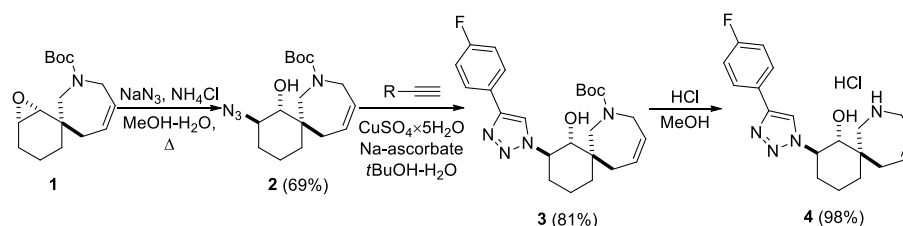


Figure 1. Pyrrole-based derivatives with anticancer activity.

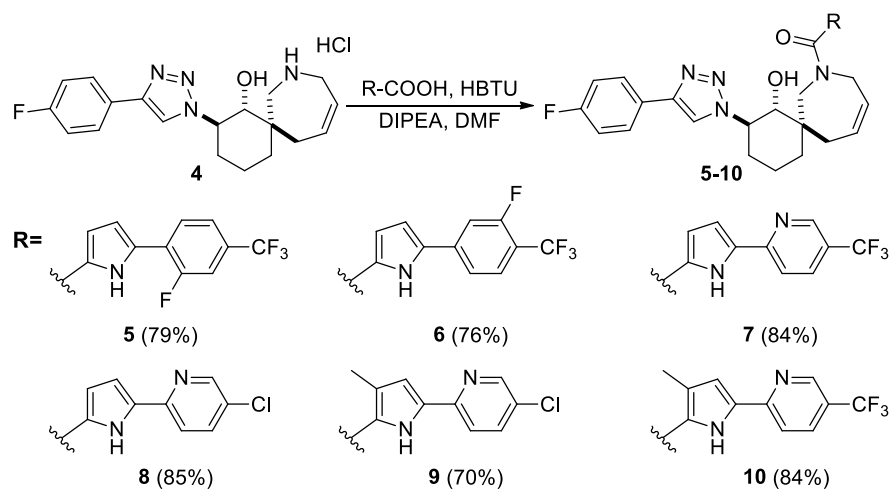
2. Results and Discussion

In a recent work, a set of spirocyclic derivatives based on 8-oxaspiro[5.6]dodecane were synthesized and profiled *in vitro* against the hNNMT target to evaluate their anti-cancer therapeutic potential [18]. Based on their synthetic pathway, the replacement of an oxygen atom with a nitrogen atom to obtain an additional point for the functionalization of spirocycles was envisioned. Therefore, a modified literature approach [18] was adopted for the production of epoxide **1** from commercially available reagents (Scheme 1). Scheme 1 shows the synthesis of 1,2,3-triazole **4**, which contains an unprotected nitrogen atom in a 7-membered ring. Azide **2** was obtained from compound **1** through the epoxide ring opening with an azide-anion. Then, 1,2,3-triazole **3** was synthesized via a “click-reaction” with the 1-ethynyl-4-fluorobenzene and using $\text{CuSO}_4 \times 5\text{H}_2\text{O}$ and Na-ascorbate. Amine hydrochloride **4** was obtained by removing the protecting group under acidic conditions. The stereochemistry of such compounds was assigned through comparison with similar structures from the literature [19].



Scheme 1. Synthesis of amine **4**.

Then, compounds **5–10** were synthesized from amine hydrochloride **4** using a coupling reaction. *N,N,N',N'*-tetramethyl-*O*-(1*H*-benzotriazol-1-yl)-uronium hexafluoro-phosphate (HBTU) was used as the activating agent, while the corresponding acids used have already been characterized and described in the literature [6,20,21]. All target compounds (**5–10**) were obtained in yields of 70–85% (Scheme 2) (see Supplementary Materials).



Scheme 2. Synthesis of compounds **5–10**.

The structure of compound 8 was confirmed by X-ray diffraction analysis (Figure 2).

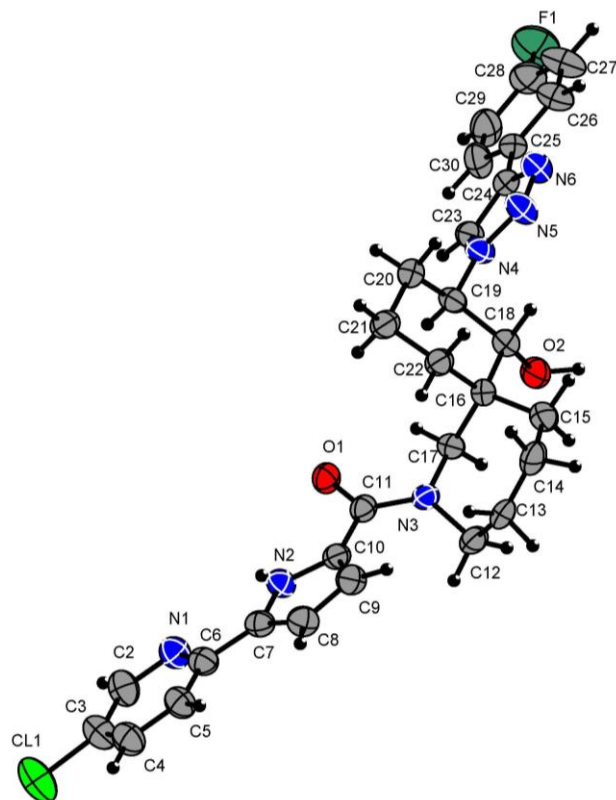


Figure 2. X-ray molecular structure of compound 8 with atom labeling. Green = fluorine atoms; red = oxygen atoms; grey = carbon atoms; blue = nitrogen atoms; black = hydrogen atoms.

3. Materials and Methods

^1H and ^{13}C NMR spectra were recorded using a Bruker Avance 400 instrument with operating frequencies of 400 and 100 MHz, respectively, and calibrated using residual undeuterated chloroform ($\delta^1\text{H} = 7.27$ ppm) and CDCl_3 ($\delta^{13}\text{C} = 77.16$ ppm) or undeuterated dimethyl sulfoxide (DMSO) ($\delta^1\text{H} = 2.50$ ppm) and DMSO- d_6 ($\delta^{13}\text{C} = 39.51$ ppm) as internal references. The following abbreviations were used to set multiplicities: s = singlet, d = doublet, t = triplet, q = quartet, m = multiplet, br = broad. The purity of the final compounds was checked through liquid chromatography–mass spectrometry (LCMS) via a Shimadzu LCMS-2010A using three types of detection systems: EDAD, ELSD and UV. High-resolution mass spectra (HRMS) were registered using a Sciex TripleTOF 5600+. We used commercial reagents and solvents without further purification. Reactions were monitored by thin-layer chromatography (TLC) performed on Merck TLC Silica gel plates (60 F254), using a UV light for visualization and basic aqueous potassium permanganate or iodine fumes as a developing agent.

3.1. General Procedure for Synthesis of Compounds 5–10

N,N-Diisopropylethylamine (DIPEA) (1 equiv.) was added to an appropriate acid (1 equiv.), followed by DMF (10 mL), and then, *N,N,N',N'*-tetramethyl-*O*-(1*H*-benzotriazol-1-yl)-uronium hexafluorophosphate (HBTU) (1 equiv.). The resulting solution was stirred for 2 min and added to a solution of appropriate amine (0.1 g, 1 equiv.) and DIPEA (1.1 equiv.) in DMF (10 mL) in a single portion. The reaction mixture was stirred overnight; DMF was evaporated, and the residue was dissolved in DCM (50 mL per 1 g of crude product) and successively washed with 5% aqueous NaOH and 10% tartaric acid solutions (25 mL per 1 g of crude product). The organic layer was dried over Na_2SO_4 , filtered and

evaporated. Crude product was purified by flash chromatography using a hexane/EtOAc mixture as an eluent (from 3:1 to 1:2) to produce the target compounds.

(5-(2-Fluoro-4-(trifluoromethyl)phenyl)-1H-pyrrol-2-yl)((1R,2R,6R)-2-(4-(4-fluorophenyl)-1H-1,2,3-triazol-1-yl)-1-hydroxy-8-azaspiro[5.6]dodec-10-en-8-yl)methanone (5)

M = 125 mg, slightly yellow powder. Yield = 79%. Rf = 0.6 in hexane/EtOAc 1:2.

$^1\text{H-NMR}$ (400 MHz, CDCl_3) δ : 1.29–1.56 (m, 2 H), 1.61–1.79 (m, 2 H), 1.98–2.16 (m, 2 H), 2.28 (d, $J = 11.8$ Hz, 1 H), 3.03 (dd, $J = 14.2, 2.1$ Hz, 1 H), 3.24 (d, $J = 14.2$ Hz, 1 H), 3.54 (t, $J = 10.7$ Hz, 1 H), 4.15 (dd, $J = 17.0, 3.1$ Hz, 1 H), 4.34 (d, $J = 14.5$ Hz, 1 H), 4.60–4.71 (m, 1 H), 4.95 (d, $J = 17.5$ Hz, 1 H), 5.15 (d, $J = 10.8$ Hz, 1 H), 5.60 (d, $J = 10.5$ Hz, 1 H), 5.80–5.90 (m, 1 H), 6.63–6.68 (m, 1 H), 6.71–6.77 (m, 1 H), 7.09 (t, $J = 8.7$ Hz, 2 H), 7.36–7.44 (m, 2 H), 7.71 (t, $J = 7.9$ Hz, 1 H), 7.79 (dd, $J = 8.6, 5.4$ Hz, 2 H), 7.89 (s, 1 H), 10.17 (br. s, 1 H).

$^{13}\text{C-NMR}$ (100 MHz, CDCl_3) δ : 20.2, 32.4, 34.5, 36.7, 47.9, 50.3, 52.3, 63.4, 78.2, 111.3 (d, $J = 4.6$ Hz), 114.1 (dq, $J = 3.9, 26.2$ Hz), 114.9, 115.7 (d, $J = 21.6$ Hz, 2 C), 120.0, 121.7 (m), 122.5 (d, $J = 11.6$ Hz), 123.6 (dq, $J = 2.4, 272.2$ Hz), 124.8, 125.7, 127.4 (d, $J = 3.3$ Hz), 127.5 (d, $J = 8.1$ Hz, 2 C), 127.7 (d, $J = 4.1$ Hz), 128.5, 128.5 (d, $J = 7.7$ Hz), 130.5 (dq, $J = 8.3, 33.5$ Hz), 146.0, 158.5 (d, $J = 250.1$ Hz), 162.6 (d, $J = 246.6$ Hz), 163.0.

IR (KBr): 3226, 2932, 2866, 1583, 1496, 1481, 1433, 1329, 1263, 1209, 1170, 1124, 791, 744 cm^{-1} .

HRMS (ESI) m/z : calcd for $\text{C}_{31}\text{H}_{29}\text{F}_5\text{N}_5\text{O}_2$ $[\text{M} + \text{H}]^+$ 598.2236, found 598.2233.

(5-(3-Fluoro-4-(trifluoromethyl)phenyl)-1H-pyrrol-2-yl)((1R,2R,6R)-2-(4-(4-fluorophenyl)-1H-1,2,3-triazol-1-yl)-1-hydroxy-8-azaspiro[5.6]dodec-10-en-8-yl)methanone (6)

M = 120 mg, white powder. Yield = 76%. Rf = 0.6 in hexane/EtOAc 1:2.

$^1\text{H-NMR}$ (400 MHz, CDCl_3) δ : 1.30–1.52 (m, 2 H), 1.60–1.76 (m, 2 H), 1.96–2.30 (m, 3 H), 2.95–3.18 (m, 2 H), 3.54 (t, $J = 10.8$ Hz, 1 H), 4.00 (d, $J = 15.2$ Hz, 1 H), 4.35 (d, $J = 14.5$ Hz, 1 H), 4.67 (t, $J = 9.6$ Hz, 1 H), 4.83 (d, $J = 17.0$ Hz, 1 H), 5.39–5.61 (m, 2 H), 5.78–5.90 (m, 1 H), 6.51 (d, $J = 2.1$ Hz, 2 H), 7.06 (t, $J = 8.6$ Hz, 2 H), 7.29–7.37 (m, 2 H), 7.51 (t, $J = 7.9$ Hz, 1 H), 7.65 (dd, $J = 8.5, 5.4$ Hz, 2 H), 7.78 (s, 1 H), 10.70 (br. s, 1 H).

$^{13}\text{C-NMR}$ (100 MHz, CDCl_3) δ : 20.2, 32.6, 34.3, 36.8, 48.0, 50.2, 52.3, 63.3, 78.1, 109.5, 112.8 (d, $J = 22.3$ Hz), 115.4, 115.6 (d, $J = 21.6$ Hz, 2 C), 116.4 (dq, $J = 12.7, 33.2$ Hz), 119.9, 120.2 (d, $J = 3.1$ Hz), 122.7 (q, $J = 271.6$ Hz), 124.9, 126.0, 127.4, 127.4 (d, $J = 8.1$ Hz, 2 C), 127.7 (dq, $J = 1.8, 4.4$ Hz), 128.3, 133.1, 137.4 (d, $J = 8.7$ Hz), 145.8, 160.1 (dq, $J = 2.2, 254.9$ Hz), 162.5 (d, $J = 246.6$ Hz), 163.1.

IR (KBr): 3214, 2933, 2864, 1627, 1582, 1495, 1484, 1435, 1323, 1213, 1127, 1041, 840, 790 cm^{-1} .

HRMS (ESI) m/z : calcd for $\text{C}_{31}\text{H}_{29}\text{F}_5\text{N}_5\text{O}_2$ $[\text{M} + \text{H}]^+$ 598.2236, found 598.2238.

((1R,2R,6R)-2-(4-(4-Fluorophenyl)-1H-1,2,3-triazol-1-yl)-1-hydroxy-8-azaspiro[5.6]dodec-10-en-8-yl)(5-(5-(trifluoromethyl)pyridin-2-yl)-1H-pyrrol-2-yl)methanone (7)

M = 128 mg, slightly brown powder. Yield = 84%. Rf = 0.5 in hexane/EtOAc 1:2.

$^1\text{H-NMR}$ (400 MHz, CDCl_3) δ : 1.28–1.56 (m, 2 H), 1.58–1.79 (m, 2 H), 1.97–2.20 (m, 2 H), 2.28 (d, $J = 11.6$ Hz, 1 H), 3.03 (dd, $J = 14.2, 2.1$ Hz, 1 H), 3.23 (d, $J = 14.4$ Hz, 1 H), 3.53 (t, $J = 10.7$ Hz, 1 H), 4.15 (dd, $J = 17.3, 3.3$ Hz, 1 H), 4.35 (d, $J = 14.5$ Hz, 1 H), 4.62–4.73 (m, 1 H), 4.95 (d, $J = 16.6$ Hz, 1 H), 5.15 (d, $J = 11.0$ Hz, 1 H), 5.58 (d, $J = 10.4$ Hz, 1 H), 5.79–5.89 (m, 1 H), 6.60–6.68 (m, 1 H), 6.75–6.82 (m, 1 H), 7.09 (t, $J = 8.7$ Hz, 2 H), 7.63 (d, $J = 8.4$ Hz, 1 H), 7.76–7.88 (m, 3 H), 7.91 (s, 1 H), 8.72 (s, 1 H), 10.57 (br. s, 1 H).

$^{13}\text{C-NMR}$ (100 MHz, CDCl_3) δ : 20.2, 32.3, 34.4, 36.7, 47.9, 50.2, 52.3, 63.4, 78.2, 109.9, 115.3, 115.7 (d, $J = 21.6$ Hz, 2 C), 118.4, 120.2, 123.7 (q, $J = 272.0$ Hz), 124.3 (q, $J = 33.2$ Hz), 124.8 (br.), 126.2, 127.4, 127.5 (d, $J = 8.1$ Hz, 2 C), 128.5, 133.2, 133.9 (q, $J = 3.3$ Hz), 146.0, 146.5 (q, $J = 4.1$ Hz), 152.1, 162.5 (d, $J = 246.6$ Hz), 163.0.

IR (KBr): 3440, 3246, 2930, 2868, 1605, 1496, 1474, 1434, 1326, 1257, 1225, 1124, 1069, 841, 755 cm^{-1} .

HRMS (ESI) m/z : calcd for $\text{C}_{30}\text{H}_{29}\text{F}_4\text{N}_6\text{O}_2$ $[\text{M} + \text{H}]^+$ 581.2283, found 581.2284.

(5-(5-Chloropyridin-2-yl)-1*H*-pyrrol-2-yl)((1*RS*,2*RS*,6*RS*)-2-(4-(4-fluorophenyl)-1*H*-1,2,3-triazol-1-yl)-1-hydroxy-8-azaspiro[5.6]dodec-10-en-8-yl)methanone (**8**)

M = 123 mg, white powder. Yield = 85%. Rf = 0.5 in hexane/EtOAc 1:2.

¹H-NMR (400 MHz, CDCl₃) δ: 1.37–1.58 (m, 2 H), 1.63–1.78 (m, 2 H), 2.07 (d, *J* = 10.7 Hz, 1 H), 2.12–2.26 (m, 1 H), 2.34 (d, *J* = 11.5 Hz, 1 H), 3.02–3.60 (m, 3 H), 4.17 (dd, *J* = 17.1, 3.7 Hz, 1 H), 4.42 (d, *J* = 14.4 Hz, 1 H), 4.69 (td, *J* = 11.1, 4.1 Hz, 1 H), 4.98–5.21 (m, 2 H), 5.60 (d, *J* = 11.7 Hz, 1 H), 5.82–5.93 (m, 1 H), 6.63–6.73 (m, 2 H), 7.12 (t, *J* = 8.7 Hz, 2 H), 7.51 (d, *J* = 8.5 Hz, 1 H), 7.64 (dd, *J* = 8.5, 2.4 Hz, 1 H), 7.84 (dd, *J* = 8.6, 5.4 Hz, 2 H), 7.94 (s, 1 H), 8.48 (d, *J* = 2.1 Hz, 1 H), 10.35 (br. s, 1 H).

¹³C-NMR (100 MHz, CDCl₃) δ: 20.2, 32.3, 34.2 (br.), 37.0 (br.), 48.0, 50.3, 52.4 (br.), 63.4, 78.1, 108.6, 115.5, 115.8 (d, *J* = 21.7 Hz, 2 C), 119.7, 120.3, 124.8, 125.3, 127.5 (d, *J* = 3.3 Hz), 127.6 (d, *J* = 8.1 Hz, 2 C), 128.4, 130.1, 133.8, 136.5, 146.0, 147.3, 148.4, 162.6 (d, *J* = 246.6 Hz), 163.2.

IR (KBr): 3435, 3223, 2933, 2864, 1584, 1560, 1496, 1457, 1433, 1295, 1257, 1219, 1074, 839, 787, 753 cm⁻¹.

HRMS (ESI) *m/z*: calcd for C₂₉H₂₉ClFN₆O₂ [M + H]⁺ 547.2019, found 547.2024.

(5-(5-Chloropyridin-2-yl)-3-methyl-1*H*-pyrrol-2-yl)((1*RS*,2*RS*,6*RS*)-2-(4-(4-fluorophenyl)-1*H*-1,2,3-triazol-1-yl)-1-hydroxy-8-azaspiro[5.6]dodec-10-en-8-yl)methanone (**9**)

M = 103 mg, white powder. Yield = 70%. Rf = 0.6 in hexane/EtOAc 1:2.

¹H-NMR (400 MHz, CDCl₃) δ: 1.35–1.56 (m, 2 H), 1.66–1.75 (m, 2 H), 2.02–2.23 (m, 5 H), 2.25–2.36 (m, 1 H), 3.04–3.23 (m, 2 H), 3.58 (t, *J* = 8.4 Hz, 1 H), 4.03 (d, *J* = 18.3 Hz, 1 H), 4.41 (d, *J* = 14.5 Hz, 1 H), 4.50–4.60 (m, 1 H), 4.65 (d, *J* = 17.7 Hz, 1 H), 5.10 (br. s, 1 H), 5.44–5.55 (m, 1 H), 5.75–5.86 (m, 1 H), 6.48 (d, *J* = 2.2 Hz, 1 H), 7.09 (t, *J* = 8.7 Hz, 2 H), 7.44 (d, *J* = 8.6 Hz, 1 H), 7.59 (dd, *J* = 8.5, 2.4 Hz, 1 H), 7.79 (dd, *J* = 8.6, 5.4 Hz, 2 H), 7.89 (s, 1 H), 8.39 (d, *J* = 1.9 Hz, 1 H), 9.82 (br. s, 1 H).

¹³C-NMR (100 MHz, CDCl₃) δ: 12.8, 20.2, 32.1, 34.5 (br.), 37.0 (br.), 48.5 (br.), 50.1, 53.9 (br.), 63.5, 78.5, 110.0, 115.8 (d, *J* = 21.7 Hz, 2 C), 119.3, 120.4, 123.4, 123.8, 125.7 (br.), 127.4 (d, *J* = 3.3 Hz), 127.5 (d, *J* = 8.1 Hz, 2 C), 127.7, 129.5, 132.2, 136.5, 146.0, 147.7, 148.2, 162.6 (d, *J* = 246.6 Hz), 165.6.

IR (KBr): 3231, 2927, 2869, 1587, 1451, 1381, 1297, 1259, 1221, 1111, 1075, 839, 813, 610 cm⁻¹.

HRMS (ESI) *m/z*: calcd for C₃₀H₃₁ClFN₆O₂ [M + H]⁺ 561.2176, found 561.2172.

((1*RS*,2*RS*,6*RS*)-2-(4-(4-Fluorophenyl)-1*H*-1,2,3-triazol-1-yl)-1-hydroxy-8-azaspiro[5.6]dodec-10-en-8-yl)(3-methyl-5-(5-(trifluoromethyl)pyridin-2-yl)-1*H*-pyrrol-2-yl)methanone (**10**)

M = 129 mg, white powder. Yield = 84%. Rf = 0.6 in hexane/EtOAc 1:2.

¹H-NMR (400 MHz, CDCl₃) δ: 1.36–1.58 (m, 2 H), 1.71–1.84 (m, 2 H), 2.06–2.24 (m, 5 H), 2.33 (d, *J* = 11.6 Hz, 1 H), 3.07–3.28 (m, 2 H), 3.60 (t, *J* = 10.5 Hz, 1 H), 4.06 (d, *J* = 18.6 Hz, 1 H), 4.43 (d, *J* = 14.4 Hz, 1 H), 4.51–4.71 (m, 2 H), 4.95 (br. s, 1 H), 5.48–5.57 (m, 1 H), 5.79–5.90 (m, 1 H), 6.61 (d, *J* = 2.3 Hz, 1 H), 7.10 (t, *J* = 8.7 Hz, 2 H), 7.58 (d, *J* = 8.4 Hz, 1 H), 7.76–7.91 (m, 4 H), 8.70 (s, 1 H), 9.87 (br. s, 1 H).

¹³C-NMR (100 MHz, CDCl₃) δ: 12.7, 20.2, 32.1, 34.6 (br.), 37.0 (br.), 48.5 (br.), 50.1, 53.9 (br.), 63.6, 78.5, 111.3, 115.8 (d, *J* = 21.6 Hz, 2 C), 118.0, 120.3, 123.8 (q, *J* = 272.0 Hz), 123.9 (q, *J* = 33.0 Hz), 123.9, 124.4, 125.7 (br.), 127.4 (d, *J* = 3.1 Hz), 127.5 (d, *J* = 8.1 Hz, 2 C), 127.9 (br.), 131.8, 133.9 (q, *J* = 3.3 Hz), 146.1, 146.4 (q, *J* = 4.2 Hz), 152.4 (d, *J* = 1.3 Hz), 162.6 (d, *J* = 246.6 Hz), 165.5.

IR (KBr): 3196, 2932, 2863, 1602, 1496, 1324, 1294, 1240, 1127, 1071, 839, 733 cm⁻¹.

HRMS (ESI) *m/z*: calcd for C₃₁H₃₁F₄N₆O₂ [M + H]⁺ 595.2439, found 595.2427.

3.2. Crystallography Details

The data of **8** were collected by using an STOE diffractometer Pilatus100K detector, with mirror-focusing collimation Cu K α (1.54086 Å) radiation, in rotation method mode. STOE X-Area software (STOE & Cie GmbH, Darmstadt, Germany, 2013) was used for cell refinement and data reduction. Data collection and image processing were performed using an X-Area 1.67 (STOE & Cie GmbH, Darmstadt, Germany, 2013). Intensity data were

scaled using LANA (part of X-Area) in order to minimize differences in the intensities of symmetry-equivalent reflections (multi-scan method).

Crystallization of molecule 8 has a tendency to form twins, and despite numerous attempts, we were unable to find a single crystal. A sample of two crystals (basf 0.49) was studied.

Under refinement of the positional and thermal parameters of the atoms, reflections from twin crystal were used, but the positions of some reflections coincided, which affected the value of the R-factor and the refinement process.

Cell parameters: $a = 9.750(1) \text{ \AA}$, $b = 10.3730(1) \text{ \AA}$, $c = 26.349(2) \text{ \AA}$, $\alpha 103.156(3)$, $\beta 96.11(1)^\circ$, $\gamma 102.875$; $V = 2649.7(4)$, $Z = 4$, $d_{\text{calc}} = 1.376 \text{ Mg/m}^3$. Crystal class is monoclinic. Space group: $P2_1/n$. Absorption coefficient: 1.662 mm^{-1} .

The structures were solved and refined using the SHELX program [22]. The non-hydrogen atoms were refined by using the anisotropic full-matrix least-square procedure.

Hydrogen atoms were placed in the calculated positions and allowed to ride on their parent atoms (C-H 0.93–0.98; Uiso 1.2 Ueq (parent atom)). The position of the hydrogen atom in the (O2-H21) hydroxy group was determined from Fourier synthesis and was freely refined in the isotropic approximation. The oxygen group O2-H21 (Figure 2) forms a hydrogen bond with the oxygen atom O1ⁱ (angle O2-H21...O1ⁱ $162(10)^\circ$, distance H21-O1ⁱ $1.83(12) \text{ \AA}$), thereby forming endless chains of molecules along the **b** axis.

Refinement was made against 25,016 reflections. A total of 363 parameters were refined using 0 restraints. The final R value was 0.107 against $8272 F^2 > 2\sigma(F^2)$. Molecular geometry calculations were performed using the SHELX program, and the molecular graphics were prepared by using DIAMOND software [23] (Brandenburg, K. DIAMOND, Release 2.1d; Crystal Impact GbR: Bonn, Germany, 2000).

CCDC-2305668 contains the supplementary crystallographic data for this paper. These data can be obtained free of charge from The Cambridge Crystallographic Data Centre via www.ccdc.cam.ac.uk/data_request/cif (accessed on 3 November 2023).

4. Conclusions

As a result of this study, we obtained the target pyrrole derivatives 5–10, the synthesis of which was validated, and the compounds were fully characterized by spectral analysis methods. The structure of 8 was also studied via X-ray diffraction analysis, which confirmed that diastereomerically pure products were obtained. The biological activity of the obtained compounds are to be explored as soon as any appropriated panel assay is available for this project.

Supplementary Materials: The following data are available online: ¹H-NMR, ¹³C-NMR, 2D correlation spectra 1H-1H (COSY, NOESY), 1H-13C (HSQC) and HR-MS of 8.

Author Contributions: Conceptualization, A.A. and A.V.K.; methodology, A.V.K.; performance of chemical synthesis, I.R.I.; registration and interpretation of NMR data and structural characterization of both compounds, I.R.I. and A.V.K.; X-ray crystallography study of the crystals, V.A.T.; writing—original draft preparation, I.R.I. and A.V.K.; writing—review and editing, V.A.T. and A.A. All authors have read and agreed to the published version of the manuscript.

Funding: The current work was financially supported by the Russian Foundation for Basic Research (Grant No. 20-33-90036).

Data Availability Statement: Data are contained within the article and supplementary materials.

Acknowledgments: This study was performed using equipment purchased at the expense of the Development Program of Moscow State University. We thank Ivan A. Godovikov for assisting with the NMR experiments. This study was conducted within the state program of the TIPS RAS.

Conflicts of Interest: The authors declare no conflicts of interest.

References

1. Chhikara, B.S.; Parang, K. Global Cancer Statistics 2022: The Trends Projection Analysis. *Chem. Biol. Lett.* **2023**, *10*, 451.
2. Barghi Lish, A.; Foroumadi, A.; Kolvari, E.; Safari, F. Synthesis and Biological Evaluation of 12-Aryl-11-Hydroxy-5,6-Dihydropyrrolo[2'',1'':3',4']Pyrazino[1',2':1,5]Pyrrolo[2,3-d]Pyridazine-8(9 H)-One Derivatives as Potential Cytotoxic Agents. *ACS Omega* **2023**, *8*, 42212–42224. [[CrossRef](#)]
3. Moghadam, E.S.; Mireskandari, K.; Abdel-Jalil, R.; Amini, M. An Approach to Pharmacological Targets of Pyrrole Family from Medicinal Chemistry Viewpoint. *Mini Rev. Med. Chem.* **2022**, *22*, 2486–2561. [[CrossRef](#)]
4. Li Petri, G.; Spanò, V.; Spatola, R.; Holl, R.; Raimondi, M.V.; Barraja, P.; Montalbano, A. Bioactive Pyrrole-Based Compounds with Target Selectivity. *Eur. J. Med. Chem.* **2020**, *208*, 112783. [[CrossRef](#)]
5. Kilic-Kurt, Z.; Bakar-Ates, F.; Aka, Y.; Kutuk, O. Design, Synthesis and In Vitro Apoptotic Mechanism of Novel Pyrrolopyrimidine Derivatives. *Bioorganic Chem.* **2019**, *83*, 511–519. [[CrossRef](#)]
6. Curreli, F.; Ahmed, S.; Benedict Victor, S.M.; Iusupov, I.R.; Belov, D.S.; Markov, P.O.; Kurkin, A.V.; Altieri, A.; Debnath, A.K. Preclinical Optimization of Gp120 Entry Antagonists as Anti-HIV-1 Agents with Improved Cytotoxicity and ADME Properties through Rational Design, Synthesis, and Antiviral Evaluation. *J. Med. Chem.* **2020**, *63*, 1724–1749. [[CrossRef](#)]
7. Li, Z.; Pan, M.; Su, X.; Dai, Y.; Fu, M.; Cai, X.; Shi, W.; Huang, W.; Qian, H. Discovery of Novel Pyrrole-Based Scaffold as Potent and Orally Bioavailable Free Fatty Acid Receptor 1 Agonists for the Treatment of Type 2 Diabetes. *Bioorganic Med. Chem.* **2016**, *24*, 1981–1987. [[CrossRef](#)]
8. Szczukowski, Ł.; Redzicka, A.; Wiatrak, B.; Krzyżak, E.; Marciniak, A.; Gębczak, K.; Gębarowski, T.; Świątek, P. Design, Synthesis, Biological Evaluation and in Silico Studies of Novel Pyrrolo[3,4-d]Pyridazinone Derivatives with Promising Anti-Inflammatory and Antioxidant Activity. *Bioorganic Chem.* **2020**, *102*, 104035. [[CrossRef](#)]
9. Motzer, R.J.; Hutson, T.E.; Tomczak, P.; Michaelson, M.D.; Bukowski, R.M.; Oudard, S.; Negrier, S.; Szczylik, C.; Pili, R.; Bjarnason, G.A.; et al. Overall Survival and Updated Results for Sunitinib Compared with Interferon Alfa in Patients with Metastatic Renal Cell Carcinoma. *J. Clin. Oncol.* **2009**, *27*, 3584–3590. [[CrossRef](#)]
10. Demetri, G.D.; Van Oosterom, A.T.; Garrett, C.R.; Blackstein, M.E.; Shah, M.H.; Verweij, J.; McArthur, G.; Judson, I.R.; Heinrich, M.C.; Morgan, J.A.; et al. Efficacy and Safety of Sunitinib in Patients with Advanced Gastrointestinal Stromal Tumour after Failure of Imatinib: A Randomised Controlled Trial. *Lancet* **2006**, *368*, 1329–1338. [[CrossRef](#)]
11. La Regina, G.; Bai, R.; Coluccia, A.; Famigliani, V.; Pelliccia, S.; Passacantilli, S.; Mazzoccoli, C.; Ruggieri, V.; Sisinni, L.; Bolognesi, A.; et al. New Pyrrole Derivatives with Potent Tubulin Polymerization Inhibiting Activity as Anticancer Agents Including Hedgehog-Dependent Cancer. *J. Med. Chem.* **2014**, *57*, 6531–6552. [[CrossRef](#)]
12. Sullivan, R.J.; Infante, J.R.; Janku, F.; Wong, D.J.L.; Sosman, J.A.; Keedy, V.; Patel, M.R.; Shapiro, G.I.; Mier, J.W.; Tolcher, A.W.; et al. First-in-Class ERK1/2 Inhibitor Ulixertinib (BVD-523) in Patients with MAPK Mutant Advanced Solid Tumors: Results of a Phase I Dose-Escalation and Expansion Study. *Cancer Discov.* **2018**, *8*, 184–195. [[CrossRef](#)]
13. Bianco, M.D.C.A.D.; Marinho, D.I.L.F.; Hoelz, L.V.B.; Bastos, M.M.; Boechat, N. Pyrroles as Privileged Scaffolds in the Search for New Potential HIV Inhibitors. *Pharmaceuticals* **2021**, *14*, 893. [[CrossRef](#)]
14. Kombarov, R.; Altieri, A.; Genis, D.; Kirpichenok, M.; Kochubey, V.; Rakitina, N.; Titarenko, Z. BioCores: Identification of a Drug/Natural Product-Based Privileged Structural Motif for Small-Molecule Lead Discovery. *Mol. Divers.* **2010**, *14*, 193–200. [[CrossRef](#)]
15. Zheng, Y.-J.; Tice, C.M. The Utilization of Spirocyclic Scaffolds in Novel Drug Discovery. *Expert Opin. Drug Discov.* **2016**, *11*, 831–834. [[CrossRef](#)]
16. Ritchie, T.J.; Macdonald, S.J.F. The Impact of Aromatic Ring Count on Compound Developability—Are Too Many Aromatic Rings a Liability in Drug Design? *Drug Discov. Today* **2009**, *14*, 1011–1020. [[CrossRef](#)]
17. Lovering, F. Escape from Flatland 2: Complexity and Promiscuity. *Med. Chem. Commun.* **2013**, *4*, 515. [[CrossRef](#)]
18. Iusupov, I.R.; Lukyanenko, E.R.; Altieri, A.; Kurkin, A.V. Design and Synthesis of Fsp3-Enriched Spirocyclic-Based Biological Screening Compound Arrays via DOS Strategies and Their NNMT Inhibition Profiling. *ChemMedChem* **2022**, *17*, e202200394. [[CrossRef](#)]
19. Iusupov, I.R.; Lyssenko, K.A.; Altieri, A.; Kurkin, A.V. (1R,2R,6R)-2-(6-Amino-9H-Purin-9-Yl)-8-Azaspiro[5.6]Dodec-10-En-1-Ol Dihydrochloride. *Molbank* **2022**, *2022*, M1495. [[CrossRef](#)]
20. Curreli, F.; Ahmed, S.; Benedict Victor, S.M.; Iusupov, I.R.; Spiridonov, E.A.; Belov, D.S.; Altieri, A.; Kurkin, A.V.; Debnath, A.K. Design, Synthesis, and Antiviral Activity of a Series of CD4-Mimetic Small-Molecule HIV-1 Entry Inhibitors. *Bioorganic Med. Chem.* **2021**, *32*, 116000. [[CrossRef](#)]
21. Curreli, F.; Belov, D.S.; Kwon, Y.D.; Ramesh, R.; Furimsky, A.M.; O'Loughlin, K.; Byrge, P.C.; Iyer, L.V.; Mirsalis, J.C.; Kurkin, A.V.; et al. Structure-Based Lead Optimization to Improve Antiviral Potency and ADMET Properties of Phenyl-1H-Pyrrole-Carboxamide Entry Inhibitors Targeted to HIV-1 Gp120. *Eur. J. Med. Chem.* **2018**, *154*, 367–391. [[CrossRef](#)] [[PubMed](#)]
22. Sheldrick, G.M. A Short History of SHELX. *Crystallogr. Sect. A Found. Crystallogr.* **2008**, *64*, 112–122. [[CrossRef](#)] [[PubMed](#)]
23. Brandenburg, K.; Berndt, M. *Diamond, Version 2.1 e*; Crystal Impact GbR: Bonn, Germany, 1999.

Disclaimer/Publisher's Note: The statements, opinions and data contained in all publications are solely those of the individual author(s) and contributor(s) and not of MDPI and/or the editor(s). MDPI and/or the editor(s) disclaim responsibility for any injury to people or property resulting from any ideas, methods, instructions or products referred to in the content.